UCBS#2008683, VOL 0, ISS 0

Water Cycle Algorithm (WCA): A New Technique to Harvest Maximum Power from PV

Muhammad Yaqoob Javed, Ali Hasan, Syed Tahir Hussain Rizvi, Annas Hafeez, Sajid Sarwar, and Achraf Jabeur Telmoudi

QUERY SHEET

This page lists questions we have about your paper. The numbers displayed at left are hyperlinked to the location of the query in your paper.

The title and author names are listed on this sheet as they will be published, both on your paper and on the Table of Contents. Please review and ensure the information is correct and advise us if any changes need to be made. In addition, please review your paper as a whole for typographical and essential corrections.

Your PDF proof has been enabled so that you can comment on the proof directly using Adobe Acrobat. For further information on marking corrections using Acrobat, please visit http://journalauthors.tandf.co.uk/production/acrobat.asp; https://authorservices.taylorandfrancis.com/how-to-correct-proofs-with-adobe/

The CrossRef database (www.crossref.org/) has been used to validate the references.

AUTHOR QUERIES

Q1 Please check if author names and affiliations have been typeset correctly and correct if inaccurate.

Q2 Please provide location of the conference.

Q3 Please provide the volume number and journal title.

Q4 Please note that numbered references have been changed to name and year references as per journal style. Please check.

CYBERNETICS AND SYSTEMS
https://doi.org/10.1080/01969722.2021.2008683

Water Cycle Algorithm (WCA): A New Technique to Harvest Maximum Power from PV

Muhammad Yaqoob Javed[a], Ali Hasan[a], Syed Tahir Hussain Rizvi[b],
Q1 Annas Hafeez[a], Sajid Sarwar[a], and Achraf Jabeur Telmoudi[c]

[a]Department of Electrical and Computer Engineering, COMSATS University Islamabad, Lahore Campus, Lahore, Pakistan; [b]Dipartimento Di Elettronica E Telecomunicazioni, Politecnico di Torino, Torino, Italy; [c]LISIER Laboratory, The National Higher Engineering School of Tunis (ENSIT), University of Tunis, Tunis, Tunisia

ABSTRACT

Renewable energy or alternative energy is extracted through renewable resources. These are considered as an alternative from conventional fossil fuel-based sources because conventional energy sources are depleting rapidly and raised concerns over increasing environmental impacts. Among many renewable sources, solar energy has a substantial part to meet the increased energy demand with reduced environmental effects. Solar irradiance and temperature are key factors upon which photovoltaic (PV) power generation depends but its optimum operating point gets affected by variation in the above-mentioned environmental factors. Finding the optimum operating point is a challenge due to the nonlinear solar behavior and varying nature of environmental conditions. To overcome these challenges, maximum power point (MPP) searching algorithms are exploited to get optimum power from the PV energy system. Maximum power point tracking (MPPT) behavior is different for various weather conditions, for instance, partial shading (PS), and uniform irradiance (UI) conditions. Numerous MPPT methods came to be used to find the optimum power. This work deals with the development of a novel technique for MPP finding of a PV system on the basis of the Water Cycle Algorithm (WCA) under PS conditions. It turns out to be good in terms of exploration and exploitation. Thus, it has the capability to avoids getting stuck in local minima (LM) and to find the global maxima (GM). The performance of the CSA technique is examined on five different types of P-V patterns for UI and PS conditions through MATLAB simulation and experimental setup. The findings of CVA are equated with the previous well-known soft computing methods such as PSO, ACS, DFO, and conventional method P&O to evaluate performance. The outcomes reveal that the WCA algorithm overtakes P&O from the perspective of robustness, accuracy, efficiency, and stability, as well as PSO in respect of converging speed and efficiency.

KEYWORDS
MPPT; partial shading condition; Perturb and Observe (P&O); photovoltaic (PV); water cycle algorithm (WCA)

CONTACT Muhammad Yaqoob Javed yaqoob.javed@cuilahore.edu.pk Department of Electrical and Computer Engineering, COMSATS University Islamabad, Lahore Campus, Lahore, Pakistan.

Introduction

Power generation from Solar is one of the most promising available renewable energy sources (RES). Which is clean, abundant, and inexhaustible of all RES to date. The sun radiates energy at the rate of 3.8×10^{20} MW and around 1.8×10^{11} MW is captured by the earth. Installed solar electricity capacity is approximately 227 GW by the end of 2015, equivalent to producing 1.9% of the electricity used globally (Renewables 2018).

Photovoltaic cells are used to convert solar energy using the principles of photovoltaic effect which is based on the interaction of light with photovoltaic materials, with absorbed photon energy greater or equal to the material's bandgap. PV energy systems have nonlinear behavior in nature and distinctive algorithm are needed to find maximum obtainable power through the PV arrays. The PV module's nonlinear features have a single MPP (Zhang et al. 2018). Solar irradiance and temperature are key factors upon which PV power generation depends. Multiple techniques have been developed to obtain optimum points and these techniques are known as MPP searching techniques. Solar irradiance is dependent on sunlight direction, shade produced by birds, clouds, buildings, and trees, etc. These partial shading conditions or fast-changing environments change MPP and thus highly affect the output power of the solar system (Aouchiche et al. 2018).

MPPT techniques may either be categorized as indirect and direct Methods. Direct approaches include procedures that measure PV current or voltage and also are independent of prior information on PV characteristics. So operating point of PV is independent of irradiance and temperature or degradation level (Karami, Moubayed, and Outbib 2017). The indirect methods are those methods that are based on parameters database including power and voltages curves of photovoltaic systems for various temperatures and irradiance, or the estimation of the MPP using mathematical functions derived through experimental data. Indirect methods use outside signals for estimation of the MPP and outside signals are typically given by measuring the short-circuit current (SCC), temperature, irradiance, and open-circuit voltage (OCV) from the PV array. MPP is derived from the monitored signal given by a set of parameters (Mohapatra et al. 2017).

MPPT methods may further be classified into classical or conventional and intelligent algorithms. Incremental Conductance (InC) and Perturb and Observe (P&O) are generally exploited conventional MPPT techniques. These techniques are fast, simple, and accurate under uniform shading conditions but their major disadvantage is that they failed to do so under PS conditions and get stuck into local maxima. Another disadvantage of this technique is that they are not efficient because they keep oscillating around MPP[4]. PV systems also employ offline techniques, for instance, fractional open-circuit voltage (FOCV) and fractional short circuit current (FSCC), which are low-cost and simple to deploy. The basic idea behind FOCV is that MPP is mostly located among 0.70 to 0.82 of the OCV and for FSCC this fraction is between 0.8 to 0.9 of the SCC (Karami, Moubayed, and Outbib 2017). The key disadvantages of these methods are that it suffers a periodic loss of power while measuring OCV or SCC and fail to perform well under PS conditions. To enhance the above-mentioned procedures, various adaptive and hybrid MPP searching approaches have been created. Under uniform and quickly varying environmental conditions, these strategies operate well, but not in PS scenarios. Furthermore, various hybrid strategies were useful in locating the MPP. In order to increase PV energy system performance, the hybrid mechanism combines traditional MPPT methods with certain optimization approaches (Harrag and Messalti 2015).

Optimization and intelligent computational approaches based on Artificial Intelligence (AI) are used to illustrate the shortcomings of traditional MPPT approaches. These techniques include Artificial Neural Networks (ANN) (Bouselham et al. 2017), Fuzzy Logic Controller (FLC) (Yilmaz, Kircay, and Borekci 2018), and Evolutionary algorithms, for instance, Particle Swarm Optimization technique (PSOT) (Babu, Rajasekar, and Sangeetha 2015), Ant Colony Optimization method (ACOM) (Ram, Babu, and Rajasekar 2017), and Genetic Algorithm (GA) (Daraban, Petreus, and Morel 2013). They may be employed on their independently or in combination with other traditional approaches. Such algorithms are complex and slow but advancement in computers give good opportunities to integrate these algorithms in real-time problems but they still have the disadvantage of not implementing in the low-cost microcontroller. So far no such method has been developed to address all these issues so we cannot say about the best technique in MPPT.

The advantage of the MPPT based on PSO presented in (Ishaque et al. 2012) is to direct calculates the duty cycle and eliminate the necessity for control loops PI. PSO method is built on an optimized search strategy that removes the limitations of traditional approaches to locate global MPPT in PS environments. But the method is complex and requires high processing power to compute. For MPPT, a neural network-based InC technique is developed (Punitha, Devaraj, and Sakthivel 2013). Artificial NN is trained through a backpropagation method to estimate online reference voltage. But required a long training time for deep networks, the complex architecture required more processing power. P&O algorithm implanted in GA and making a single algorithm result in reduced algorithm parameters and required less iteration for MPPT (Daraban, Petreus, and Morel 2014).

This research work presents a new nature-inspired metaheuristic algorithm used to find MPPT. Many studies have been conducted utilizing WCA to solve various optimization challenges. WCA was exploited by Navid Ghaffarzade in (Ghaffarzadeh 2015) to improve the variables of power system stabilizers that are exploited to reduce the oscillations of the power system. In (Haroon and Malik 2017), the authors applied WCA to hydrothermal coordination problems to get their optimum mutual operation.

The proposed solution is an indirect method of MPPT, a population-based, nature-inspired met heuristic optimization algorithm for resolving different optimization issues. The WCA is a technique motivated by nature and based on a hydrologic cycle that how water flows in streams and then streams flows into rivers and then finally downhill location into a sea (optimum point) (Eskandar et al. 2012). The best raindrop is picked through the sea, followed by some other fine raindrops in the form of rivers, and finally all rest as streams. The performance of an MPPT technique is based on accuracy, convergence speed and steady-state error, complexity, number of sensors used, and robustness and the proposed WCA technique can find the optimum point while fulfilling the above-mentioned criteria (Ghaffarzadeh 2015). The main advantages of the WCA are summarized as follow:

- It needs less Number of Function Evaluations (NFEs = No. of Iterations*Initial Population) to successfully track global MPP under partial shading and dynamic environmental conditions.
- Once comes to steady-state it does not oscillate around the MPP so power loss is prevented.
- It has a very low computational cost so, it could be executed in a low-cost microcontroller.
- It needs relatively less time to track MPP than other intelligent techniques i.e. its convergence speed is high.

Partial Shading Problem

PV arrays consist of series or parallel PV modules or a combination of both. In the open atmosphere, some modules likely experience different irradiance than other modules in the array, and this uneven irradiance on different modules is referred to as Partial shading conditions (PSC). PS happens because of the shade of the neighboring building, trees, or clouds. Modules receiving high irradiance levels can be referred to as insolated modules and modules receiving low irradiance levels can be referred to as shaded modules. In series joined PV modules, shaded modules provide less

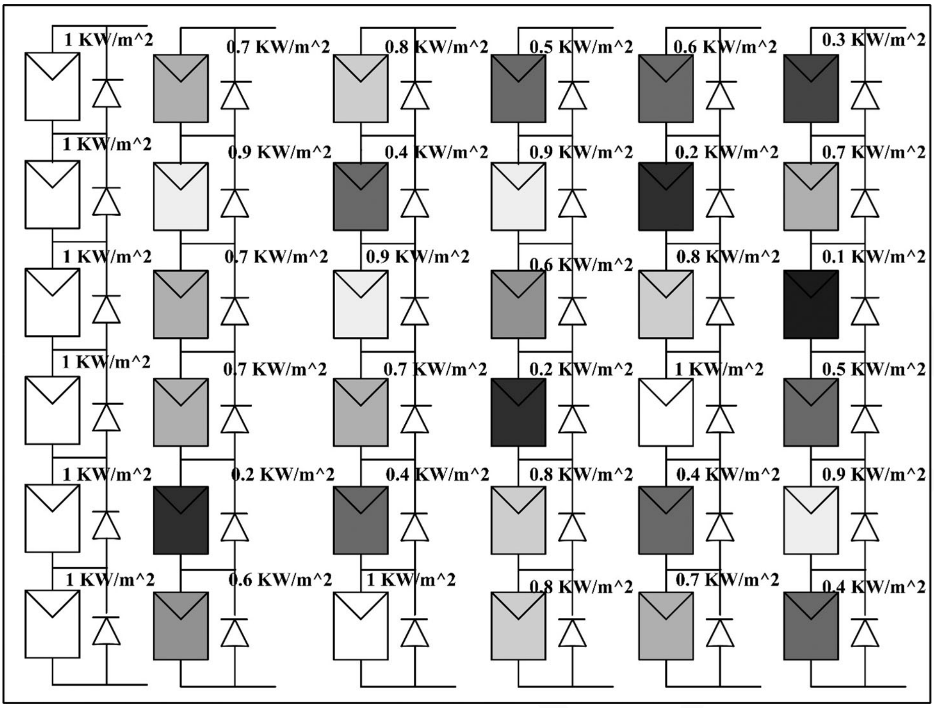

Figure 1. Series connected PV modules with by-pass diodes.

current than insolated modules. So the insolated modules drive the current in the array. A current larger than the PS module's current travels via the shaded module's shunt resistance, resulting in a negative voltage around the shaded modules and consume power rather than generate energy. This situation adversely affects the performance and efficiency of the PV system and damage PV models by creating hotspots and eventually damaging the modules because the shaded PV module behaves like a power sink and excess power dissipation in the module can irreparably damage the plastic cell encapsulation. To evade this situation, bypass diodes are linked in series with modules to provide an extra channel for current to flow, and thus improving the efficiency (Ghasemi, Foroushani, and Parniani 2016). Figure 1 shows five series-connected PV modules below UI and PS scenarios. Under UI all diodes operate in reverse biased so have no voltage drop but under different irradiance levels diode connected with shaded modules operates in forwarding bias causing the current to pass through the by-pass diode and thus experiencing a voltage drop.

In this study, a PV model has been developed and proposed WCA-based MPPT technique and one of the other well-known soft computing technique PSO was fed with identical models, and a comparative study was conducted for UI and various PS schemes. The results suggest that WCA outperforms than PSO algorithm for convergence speed.

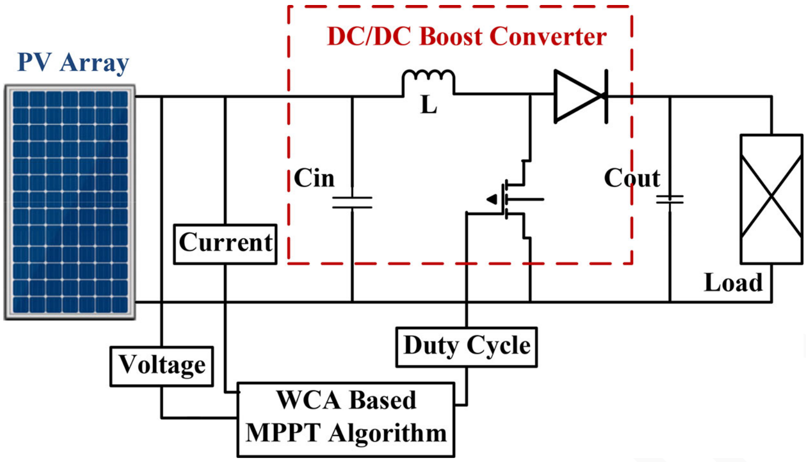

Figure 2. PV Model.

Modeling of PV System

A complete PV model is shown in Figure 2. The load is being fed by a boost converter and is being governed by a WCA-based MPP tracking controller. Several models have been established to simulate the properties of photovoltaic cells. A model of the single diode is employed for simulation.

Single Diode Model PV Module

A diode can be utilized to model the PV cell characteristics as demonstrated in Figure 3. Ideally, a PV cell may be denoted by a diode and a source of current. However, the practical model can also be realized by incorporating two resistances R_S and R_{SH} into an ideal model, which accounts for the leakage current inside the PV cell and on the borders. Practically, the model is a fair tradeoff among simplicity and accuracy The calculated equations of practical models are as given below:

$$I = I_{ph} - I_0 \exp\left(\left(\frac{q(V + IR_s)}{AKT}\right) - 1\right) - \frac{V + IR_s}{R_{SH}} \tag{1}$$

$$I_{ph} = (I_{ph,n} + K_I \Delta_T)\frac{G}{G_n} \tag{2}$$

$$I_0 = I_{0,n}\left(\frac{T_n}{T}\right)^3 \exp\left[\frac{qE_g}{ak}\left(\frac{1}{T_n} - \frac{1}{T}\right)\right] \tag{3}$$

where I_{ph} is light generated current, I_0 represents the saturation current of the diode, q denotes the electronic charge and their value is taken $(1.6 \times 10^{-19}$ C), K describes the Boltzmann constant,T illustrates the temperature, and the ideality factor of a diode represents by A that usually has a value between 1 and 1.5 [19]. $I_{ph,n}$ depicts the light- originated current at

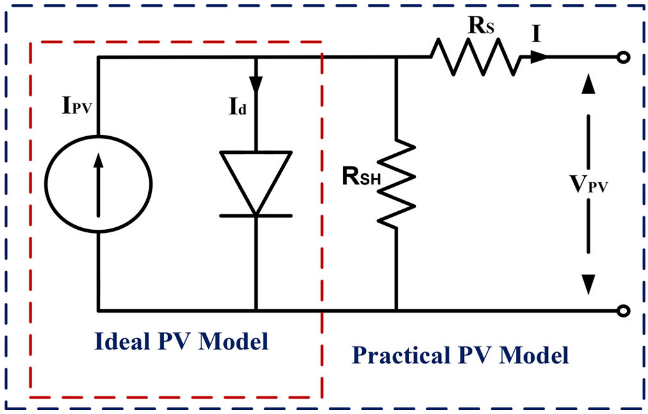

Figure 3. Diagram illustration of Single Diode PV model.

standard testing condition (STD) normally considered temperature at 25 °C and G of 1000 W/m2, and $\Delta T \ = T - Tn$ (T_n and T presents the nominal and actual temperatures [in Kelvin], correspondingly). Where E_g reveals the semiconductor's bandgap energy.

Boost Converter

Boost converter's 'D' is the primary control method for regulating the voltage V_{pv} of the selected PV array. It is an important part of the PV system to work V_{pv} at GM. An input or primary side inductor (L_i), a switch (IGBT/MOSFET), a diode, and output or secondary side (C_o) capacitor are represented in Figure 4. The mathematical relation for duty cycle is given as:

$$\frac{V_{bt}}{V_{pv}} = \frac{I_{bt}}{I_{pv}} = \sqrt{\frac{R_o}{R_{in}}} = \frac{1}{1-D} \tag{4}$$

Here, V_{bt} and I_{bt} represents the output voltage and current respectively of the power boost converter. I_{pv} *and* V_{pv} denotes the current and voltage of the PV module correspondingly.

Water Cycle Algorithm (WCA)

Basic Concept: For tackling optimization issues, a population-based optimization method is used. The WCA is a technique motivated by nature and based on a hydrologic cycle that how water flows in streams and then streams flows into rivers and then finally downhill location into a sea (optimum point). To understand it further, consider how water evaporates into the atmosphere and condenses into a colder environment, and then comes back to earth in rainfall. This water together with snowmelt starts its

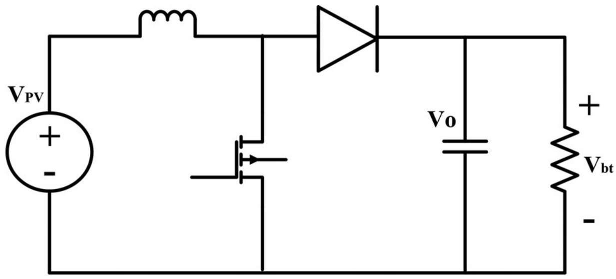

Figure 4. Basic Boost converter diagram.

journey up into the mountains through small streams which make up rivers and then finally end up into the sea. The best raindrop is designated by means of sea, while some further superb drops of rain are recognized by way of rivers. and all others are chosen as streams. Water Cycle Algorithm can find the maxima or minima of a function with good speed and accuracy (Sadollah et al. 2015).

Figures 5 and 6 show a real-world example of the Hydrological process and schematic view of the process respectively.

WCA for MPPT

MPP tracking using WCA is started by generating randomly generating voltage sample using the below equation:

$$V^i = LB + rand \times (UB - LB) \qquad i = 1, 2, \ldots, N_{pop} \tag{5}$$

$$V^i = \begin{bmatrix} V^1 \\ V^2 \\ \vdots \\ V^{Npop} \end{bmatrix} \tag{6}$$

Then calculate the power against each voltage point.

$$P^i = \begin{bmatrix} P^1 \\ P^2 \\ \vdots \\ P^{Npop} \end{bmatrix} \tag{7}$$

The initial population of the voltage points is then referred to as streams, river, and sea which are current position, local and global best voltage points based on the power at corresponding voltage points measured from PV array. A specific number of current-voltage points are directly compared with local and global best points based on the following equation:

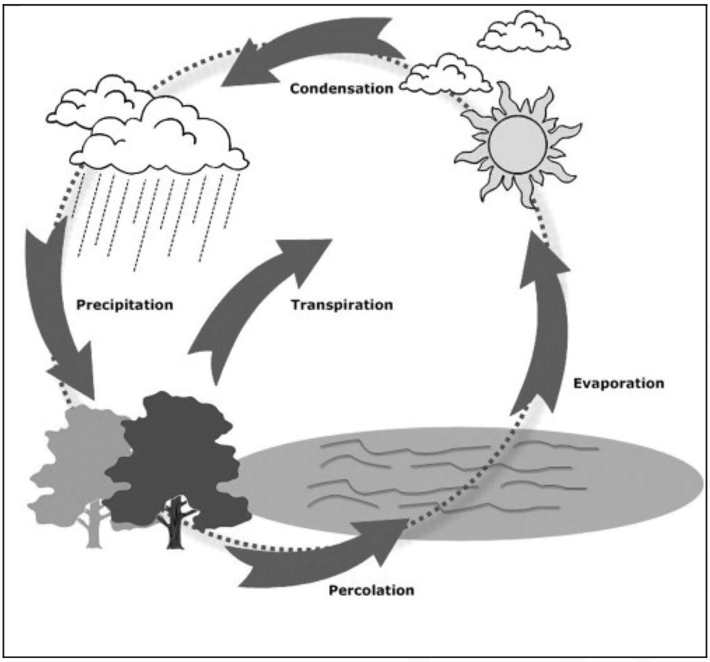

Figure 5. Hydrological Cycle.

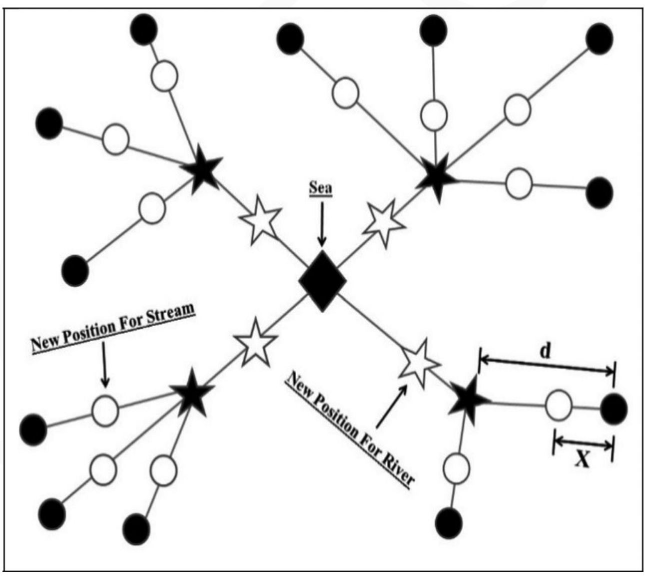

Figure 6. Schematic View of WCA.

$$NS_n = round\left\{ \left| \frac{P_n}{\sum_{i=1}^{N_{sr}} P_i} \right| \times V_{stream} \right\} \tag{8}$$

Here, NS_n presents the number of individual or streams voltage points being compared with local as well as global best points, N_{sr} and V_{stream} are

Table 1. Pseudo code of WCAfor MPPT.

1: Sense V_{pv}, I_{pv}
2: Initilaze $N_{\mathrm{var}}, N_{pop}, dist, \max_{iter}, N_{sr}$
3: Randomly generate N_{pop} voltage points and calculate power $P(V^{i}_{Npop})$
4: Create individual, local and globals best points marked as streams, river and sea respectively
5: Designate streams to rivers and sea by $NS_n = round\{\lvert \frac{P_n}{\sum_{i=1}^{N_{sr}} P_i} \rvert \times V_{stream}\}$
6: $for\ \ i = 1 : \max_{iter}$
7: %Moving streams to sea
8: $for\ \ i = NS_{sea}$
9: generate $V^{i+1}_{stream} = V^{i}_{stream} + rand \times C \times (V_{sea} - V^{i}_{stream})$
10: calculate $\mathrm{P}(V^{i+1}_{stream})$
11: $if\ \ (P(V^{i+1}_{stream}) > P(V_{sea}))$
12: $V_{sea} = V^{i+1}_{stream}$ $end\ \ end$
13: %Moving streams to rivers
14: $for\ \ \mathrm{m} = 1 : N_{sr} - 1$
15: for $\mathrm{k} = \mathrm{NS}^{k}_{river}$
16: generate $V^{k+1}_{stream} = V^{k}_{stream} + rand \times C \times (V^{m}_{river} - V^{k}_{stream})$
17: calculate $\mathrm{P}(V^{k+1}_{stream})$
18: $if\ \ (P(V^{k+1}_{stream}) > P(V^{k}_{river}))$
19: $V^{m}_{river} = V^{k+1}_{stream}$ end
20: $if\ \ (P(V^{m}_{river}) > P(V^{i}_{sea}))$
21: $V_{sea} = V^{k}_{river}$ end
22: $end\ \ end$
23: %moving rivers to sea
24: $for\ \ j = 1 : N_{sr} - 1$
25: generate $V^{j+1}_{river} = V^{j}_{river} + rand \times C \times (V_{sea} - V^{j}_{river})$
26: calculate $\mathrm{P}(V^{j+1}_{river})$
27: $if\ \ (P(V^{j+1}_{river}) > P(V_{sea}))$
28: $V_{sea} = V^{j+1}_{river}$ $end\ \ end$
29: %Evaporation condition and raining process
30: $if\ \ (\lvert V_{sea} - V^{j}_{river}\rvert < d_{\max}\ \lvert$ OR $\lvert V_{sea} - V^{i}_{stream}\rvert < d_{\max})$
31: generate new streams using Eq. (5) end
32: $new_{sea} = V_{sea}$
33 : end
34 : $Optimum\ \ Voltage$ point $= new_{sea}$
35 : $Calculate\ \ duty\ \ cycle$

the total no. of local and global best points and the total number of current-voltage points.

The pseudo-code and flow chart of this technique are shown in Table 1 and Figure 7 respectively.

The step size of the voltage points is defined by

$$V^{i+1}_{stream} = V^{i}_{stream} + rand \times C \times (V^{i}_{sea} - V^{i}_{stream}) \quad C>1 \tag{9}$$

$$V^{i+1}_{stream} = V^{i}_{stream} + rand \times C \times (V^{i}_{river} - V^{i}_{stream}) \quad C>1 \tag{10}$$

$$V^{i+1}_{river} = V^{i}_{river} + rand \times C \times (V^{i}_{sea} - V^{i}_{river}) \quad C>1 \tag{11}$$

V_{river} and V_{sea} are the local and global best points and V_{stream} are the current-voltage points. C is constant and if its value is more than one, then streams might flow in separate directions toward the river and the sea.

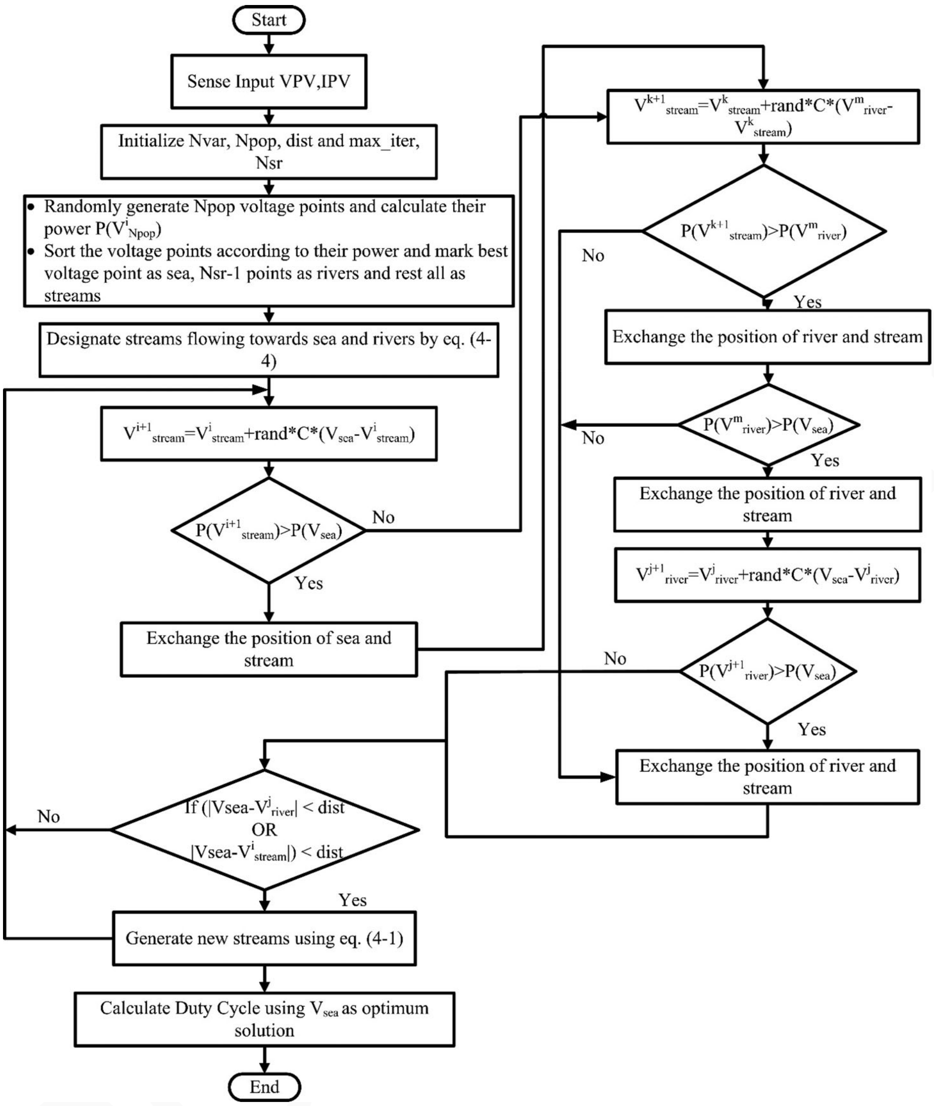

Figure 7. Flowchart of WCA based MPP Tracking.

The maximum power giving global optimum voltage point is discovered by comparing power. The position of the local best point is marked as river and the global best point is assigned as the sea in favor of a particular iteration. The individual or streams voltage points are impacted by global and local best points in subsequent iterations, and its step size is computed using Eqs. (21)–(23). The voltage at each point is located at a different location due to the step size. All the points converging into the global or sea best point with each repetition. The distance among the streams and sea comes closer to zero when the streams converge toward the MPP. To

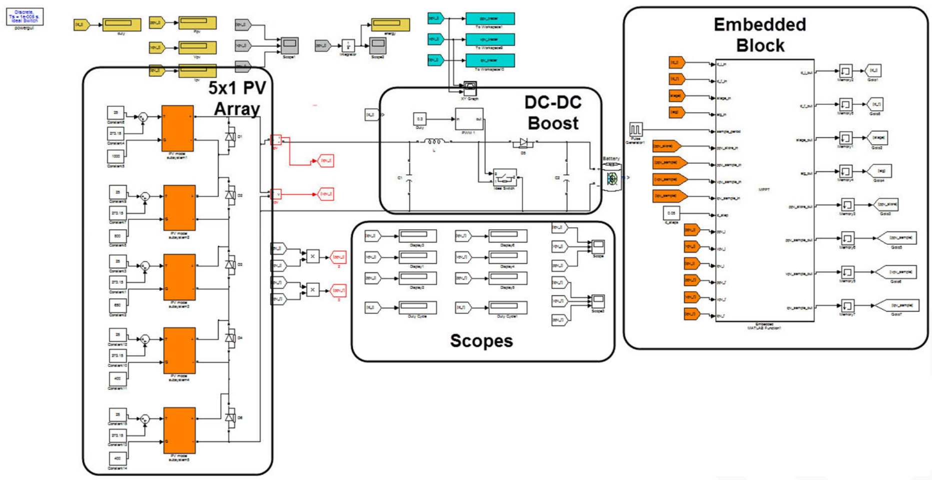

Figure 8. MATLAB/Simulink Simulation Setup.

avoid the algorithm getting stuck in the local best point a step size tolerance may be set as given below:

$$\left|V_{sea}^{i} - V_{river}^{i}\right| < dist \quad i = 1, 2, 3, \ldots, N_{sr} - 1 \tag{12}$$

$$\left|V_{sea}^{i} - V_{stream}^{i}\right| < dist \quad i = 1, 2, 3, \ldots, NS_{sea} \tag{13}$$

Whenever the distance within the sea and a river, or sea and a stream, is below tolerance, the stream or river has entered the sea and has reached its optimal point. Then as per evaporation and precipitation phenomena, new voltage points (streams and rivers) are formed by using Eq. (19) and replaced existing streams and rivers. A larger value d_{max} decreases the search radius, whereas a small number pushes the search to be closer to the optimal point. The value for *dist* adaptively decreases as:

$$dist^{i+1} = dist - \frac{dist^{i}}{\max\ iter} \tag{14}$$

dist is also used as the convergence or termination criteria.

Results

Simulation Setup

MATLAB/Simulink Simulation Setup is presented in Figure 8 describes the most commonly used PV system in which the MPPT technique is implemented (Villalva et al. 2009). The setup consists of 5 series-connected solar modules and their specification is:

$P_{mpp} = 200\,W$, $I_{mpp} = 7.6\,A$, $V_{mpp} = 26\,V$, $I_{sc} = 8.21$, $V_{oc} = 32.9\,V$. The simulation setup is used to simulate and evaluate the performances of WCA, PSO, and P&O based MPP searching techniques through various PS

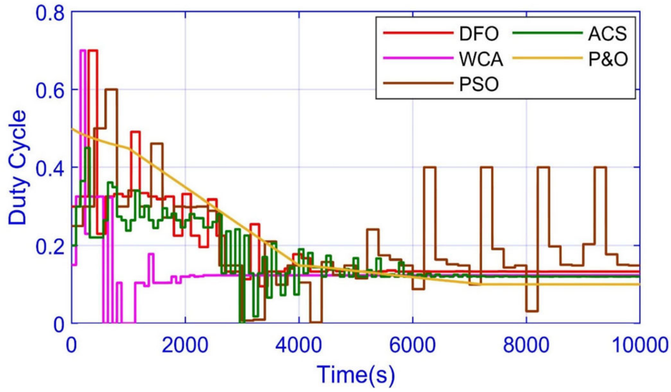

Figure 9. Case 1: Duty cycle comparability of WCA.

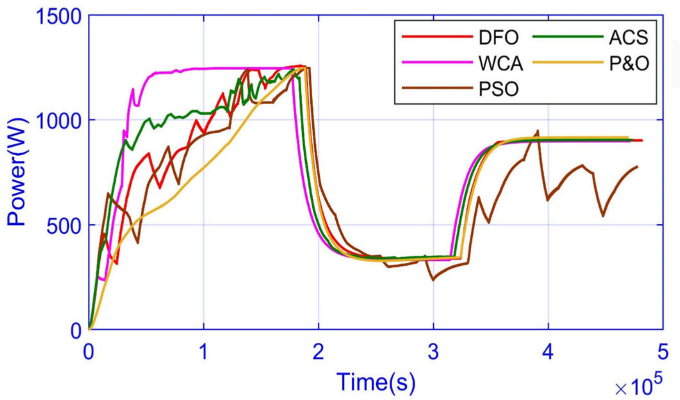

Figure 10. Case 1: Power comparability of WCA.

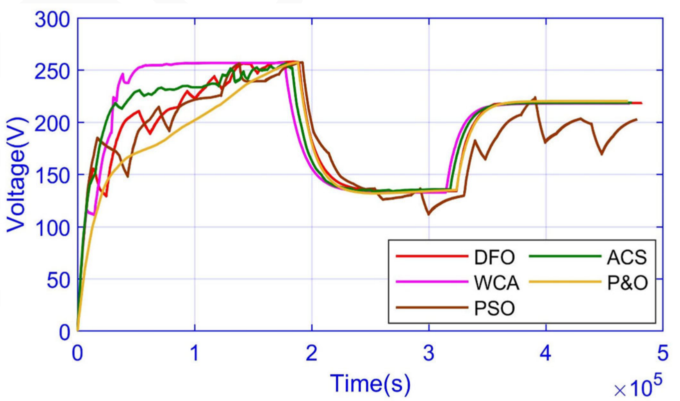

Figure 11. Case 1: Voltage comparability of WCA.

conditions. Among the battery load and PV array, the boost converter is utilized to get the required voltage as per the duty cycle. MPPT technique is implemented in the embedded block and it takes V_{pv} and I_{pv} as inputs

COLOR Online / B&W in Print

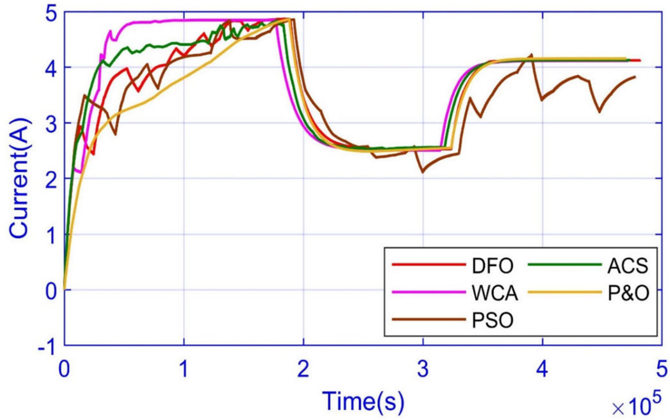

Figure 12. Case 1: Current comparability of WCA.

COLOR Online / B&W in Print

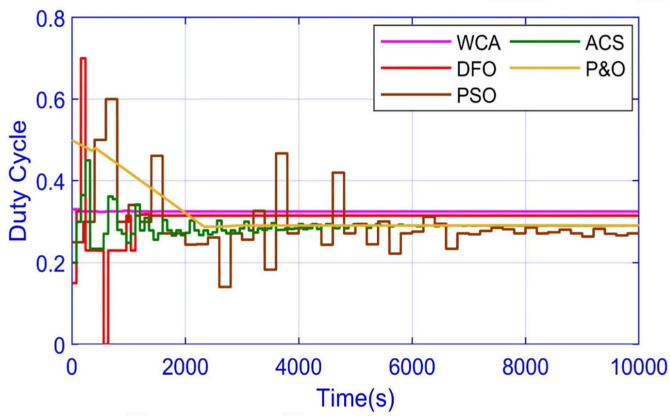

Figure 13. Case 2. Duty cycle comparability of WCA.

and D as output. Boost converter components values calculations are also an important step that is worked out in (Miyatake et al. 2011). Component values are as follows: $C_{in} = 10\,uF$, $C_{out} = 47\,uF$, $L = 200\,uH$, $F_{sw} = 20\,kHz$.

The proposed technique has been tested for UI and various PS techniques to check the accuracy and robustness. Case 1 shows the study of the CVA through UI conditions in which the irradiance level is 1000 W/m^2 for all 5 series-connected PV modules. Figure 13 shows the searching behavior of WCA under uniform shading conditions. The proposed algorithm detects the global maximum in just 28 NFEs (Number of Functions evaluations = Initial population × number of iterations) but due to the raining process, it again initializes random voltage points to search for the global maximum to avoid getting stuck in the local maximum until the stopping criteria have been fulfilled. So the total time required to find and achieve a steady state is 76 ms for WCA and 232 for PSO in case 1. For uniform irradiance, searching behavior and time required to detect for all

Table 2. Comparison of WCA with different partial shading algorithms.

Methods	Irradiance scheme	Convergence time (s)	Settling time (s)	GM existed	GM power	Tracking power	Obtained energy	Efficiency (%)
WCA	Case1	0.17	0.20	Yes	1260	1259.3	1.66×10^3	99.8
	Case2	0.20	0.38	Yes	450	449.3	0.86×10^3	99.7
	Case3	0.20	0.25	Yes	796	794.7	1.56×10^3	99.8
	Case4	0.21	0.20	Yes	520	519.5	0.88×10^3	99.8
DFO	Case1	0.23	0.27	Yes	1260	1259.1	1.66×10^3	99.8
	Case2	0.26	0.43	Yes	450	449	0.85×10^3	99.6
	Case3	0.19	0.21	Yes	796	794.4	1.55×10^3	99.7
	Case4	0.22	0.21	Yes	520	519.2	0.87×10^3	99.7
PSO	Case1	0.47	0.70	Yes	1260	1257	1.64×10^3	94.6
	Case2	0.41	0.81	Yes	450	443	0.84×10^3	97.6
	Case3	0.68	0.71	Yes	796	791.4	1.48×10^3	99.4
	Case4	0.65	0.67	Yes	520	518.7	1.41×10^3	99.7
P&O	Case1	0.33	0.71	No	1260	1210	0.97×10^3	96.1
	Case2	0.22	0.35	Yes	450	440	1.23×10^3	97.7
	Case3	0.45	0.84	No	796	580	0.73×10^3	72.9
	Case4	0.45	0.91	Yes	520	511.3	1.39×10^3	98.2
ACS	Case1	0.47	0.64	Yes	1260	1239	1.07×10^3	98.3
	Case2	0.30	0.49	Yes	450	443	1.35×10^3	98.4
	Case3	0.39	0.81	Yes	796	790.6	1.49×10^3	99.3
	Case4	0.31	0.72	Yes	520	516.7	1.42×10^3	99.4

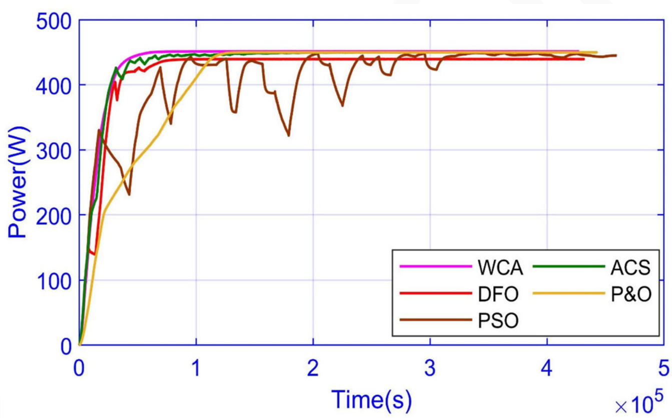

Figure 14. Case 2: Power comparability of WCA.

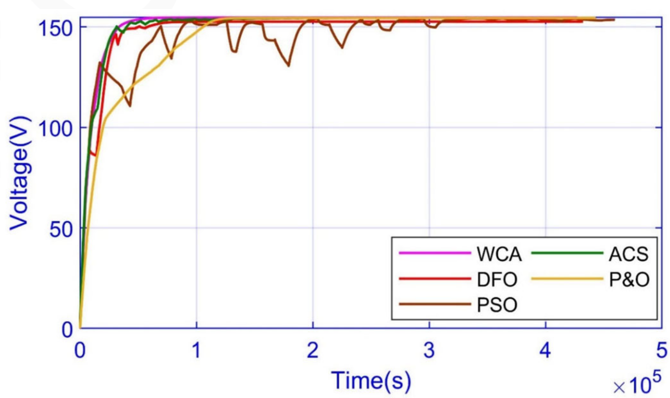

Figure 15. Case 2: Voltage comparability of WCA.

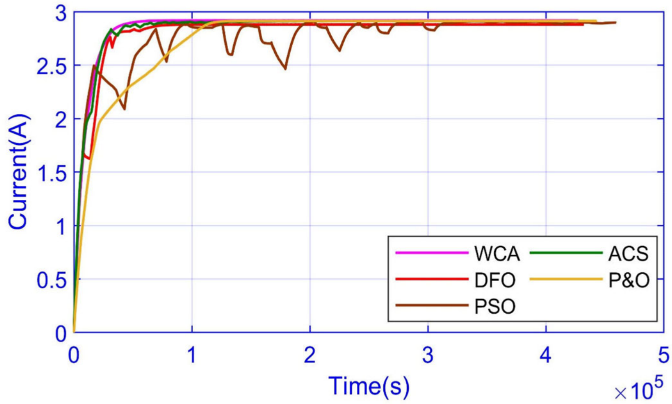

Figure 16. Case 2: Current comparability of WCA.

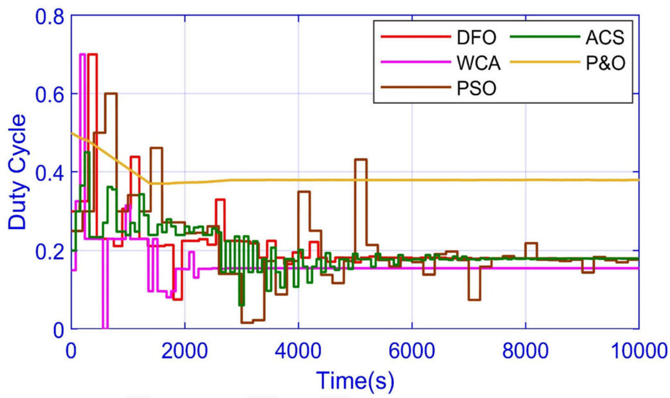

Figure 17. Case 3: Duty cycle comparability of WCA.

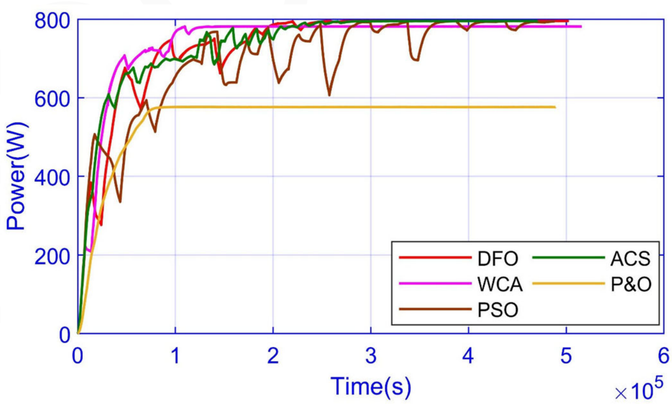

Figure 18. Case 3: Power comparability of WCA.

presented techniques are given in Figures 9 and 10. WCA is much more suitable to find global maxima than PSO because once it gets close to maxima it generates some more voltage points to ensure that the algorithm doesn't get stuck in local maxima. So the probability of WCA getting stuck in local maxima is much less than PSO which lacks exploration phenomenon and takes more time to get to global maxima. Power–time and Voltage-Time curves are shown in Figures 11 and 12 shows the searching behavior and time required to find the global maxima under partial shading techniques.

Figure 13 shows the searching behavior of WCA under shading conditions. The proposed algorithm detects the global maximum in just 28 NFEs (Number of function estimates = Initial population × number of iterations) but due to the raining process (exploration), it again initializes random voltage points to search for the global maxima to avoid getting stuck in local maxima until stopping criteria have been fulfilled, while it takes 127 NFEs for PSO to reach MPP. So the total time required to find and achieve a steady state is 76 ms for WCA and 232 for PSO while P&O is quite fast and achieve GM in only 19 ms but it does not comes to a steady-state and keeps on oscillating which results in lower efficiency in case 1. For uniform irradiance, Power and Voltage Vs time (searching behavior) for all presented techniques are shown in Figures 9 and 10. WCA is much more suitable to find global maxima than PSO because once it gets close to maxima it generates some more random voltage points to ensure that the algorithm doesn't get stuck in local maxima. Therefore, the probability of WCA being stuck in local maxima is very less than PSO, which lack exploration phenomenon and take more time to get to global maxima. Under partially shading conditions P&O does not track GM but gets stuck in local minima. Power–time and Voltage-Time curves are shown in Figures 11 and 12, which describe the searching behavior and time, required to search the GM under PS techniques.

Table 2 shows the time taken to reach the global maxima and maximum power obtained by WCA, PSO, and P&O under different irradiance conditions studied in this research. The accuracy of the WCA and PSO is the same. WCA takes 76–95 ms, PSO takes 211–304 ms to reach the GM. P&O is very fast but cannot find GM. WCA presents better efficiency results as compare to PSO and P&O, WCA shows an average of 9.81% efficiency while PSO and P&O show an average of 99.67% and 62.84% efficiencies respectively. Power-Time curves of WCA under different irradiance conditions are shown in Figures 13–17. While the graphical presentation of convergence time and efficiencies of the WCA, PSO, and P&O for all uniform and partial shading cases demonstrated in Figures 18 and 19.

Case 1 (Fast Changing Irradiance)

In this situation, entire PV modules have the same irradiance with rapid changing irradiance to time and their irradiance scheme is presented in Table

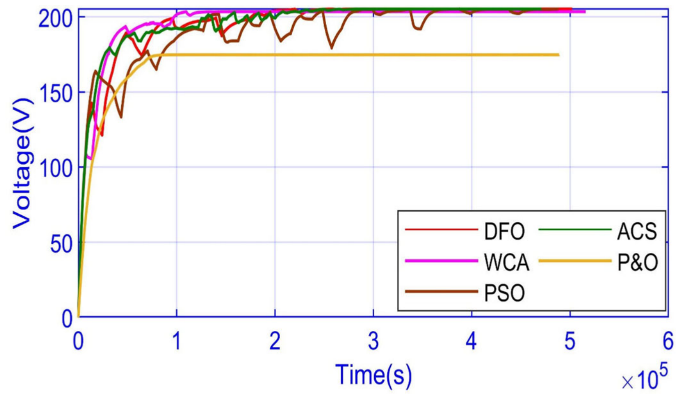

Figure 19. Case 3: Voltage comparability of WCA.

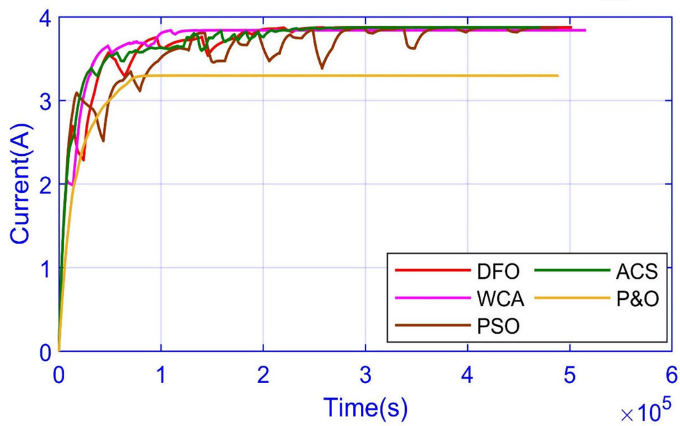

Figure 20. Case 3: Current comparability of WCA.

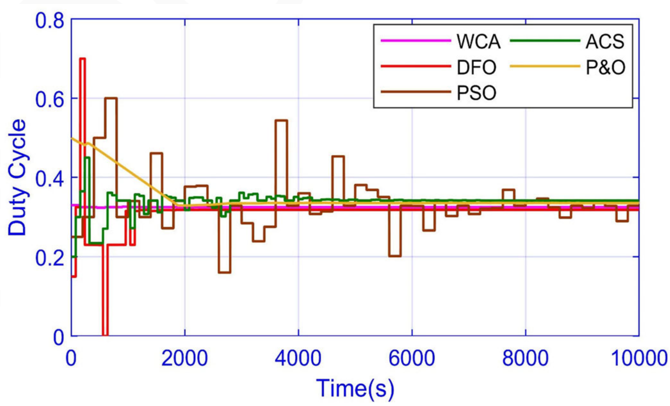

Figure 21. Case 4: Duty cycle comparability of WCA.

2. During the first interval, the power achieved by WCA is 1259.3 W as associated with 1259.1 W by DFO, 1257 W by PSO, 1239 W by ACS and 1210 W by P&O. WCA achieve 99.98% power-convergence efficacy in the first

COLOR Online / B&W in Print

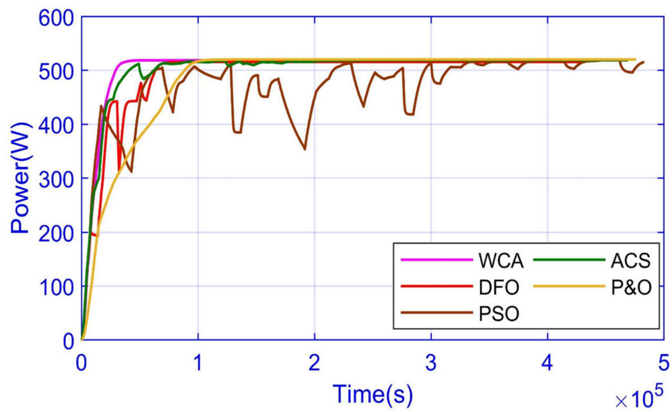

Figure 22. Case 4: Power comparability of WCA.

COLOR Online / B&W in Print

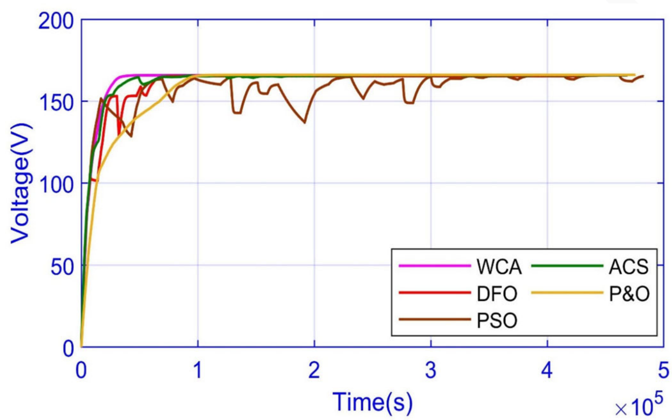

Figure 23. Case 4: Voltage comparability of WCA.

COLOR Online / B&W in Print

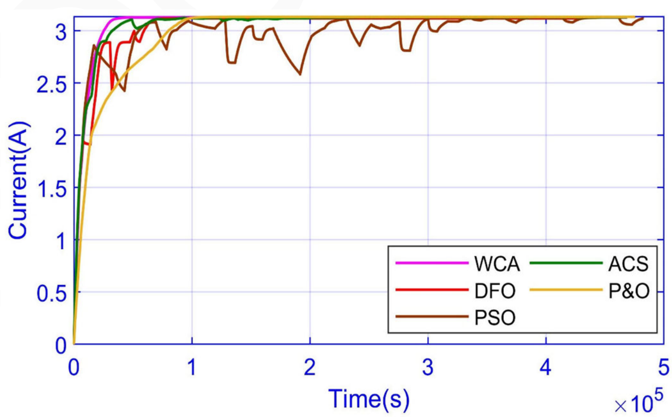

Figure 24. Case 4: Current comparability of WCA.

interval. Case 1 has three different regions reliant upon the irradiance magnitude. The average powers attained by WCA, DFO, PSO, ACS, and P&O are 830.9 W, 828.1 W, 825.1 W, 823.1 W and 819.4 W, respectively. It specifies that the maximum average is attained by WCA. The average efficiency attained by the WCA, DFO, PSO, ACS, and P&O is 99.27%, 97.96%, 97.91%, 97.95%, and 98.79%. Consequently, the techniques can be hierarchical as WCA > DFO > PSO > ACS > P&O. The calculated tracking time of WCA, DFO, PSO, ACS, and P&O is 0.17 s, 0.18 s, 0.46 s, 0.47 s, and 0.33 s, similarly. Settling time of WCA, DFO, PSO, ACS and P&O is 0.24 s, 0.25 s, 0.39 s, 0.64 s, 0.71 s, correspondingly. The control parameter is the duty-cycle which is present in Figure 9 respectively. WCA successfully reduces the magnitude of the oscillation to is less than or equal to 1 W, achieving a 94.99% decrease in the magnitude of fluctuations. Figure 10 indicates that PSO has the maximum fluctuations. ACS can harvest haphazard oscillations. The voltage and current transient are present in Figures 11 and 12 correspondingly.

Case 2 PS (Scenario I)

In this scenario, the GMPP is at 450 W. The D, P, V, and I comparability are presented in Figures 13–16 respectively. ACS and PSO show the maximum level of randomness. Settling times of ACS, PSO is large compare to WCA.Proposed technique has less oscillation in the steady-state at GMPP. The power obtained by WCA, DFO, PSO, ACS, and P&O 449.3 W, 449 W, 448 W, 443 W, and 449.5 W respectively. WCA has 99.64% efficiency as compared to DFO 99.43%, PSO 99.35%, ACS 97.93%, and P&O has 99.90%. Robustness of MPP tracking revealed by fast searching of global maxima and effective settling time at global maxima. Experimental simulations shows that it takes WCA 0.17 s, D.FO 0.19 s, P.SO 0.68 s, ACS 0.30 s and P&O 0.22 s on average and can settle after 0.55 s, 0.61 s, 0.45 s, 0.49 s and 0.35 s correspondingly. The voltage comparison result is presented in Figure 15. Stable voltage and current produced by WCA is shown in Figures 15 and 16.

Case 3 PS (Scenario II)

In this scenario the GMPP is at 796.0 W. Results for power are displayed in Figure 18 and controlled delivered by the D is presented in Figure 17. Voltage and current are illustrated in Figures 19 and 20 respectively. Under PS, the MP found by WCA, DFO, PSO, ACS, and P&O are 794.7 W, 794.4 W, 785 W, 794.6 W and 580 W, respectively.

WCA achieved the highest efficiency which is 99.67%, DFO 99.54%, while the lowest efficiency achieved by P&O which is close to about 49.40% which is LM1. The tracking time of WCA is 0.175 s, dragonfly 0.180 s, PSO 0.410 s, ACS 0.390 s and P&O 0.45 s, their settling time is 0.40 s, 0.46 s, 0.56 s, 0.81 s and 0.84 s. In harvesting global maxima, WCA stands close to DFO by 12.0 ms. WCA settle at global maxima inside

455 ms achieving 19.0% faster tracking. Faster tracking improves robustness and eliminates unwanted fluctuations. WCA attains 1–4% improved efficiency of power conversion with the ripple being <1 W and decreases the fluctuations to zero in the later phases of the iterative cycles. Under WCA, the output is steady, and its voltage and current have almost no fluctuations as present in Figures 19 and 20. In Figure 17, 'D' updating at every iteration demonstrates that WCA can sense and converge to Global Maxima in fewer iterations in appraisal to competing techniques.

Case 4 PS (Scenario III)

In this scenario, GMPP is at 520 W. The comparability is present in Figure 21 for duty-cycle. The ACS and PSO have shown extreme randomness due to random step size increments in the duty cycle. Results for power, voltage, and current are presented in Figures 22–24 respectively. Under the PS the extreme power gained by the WCA, DFO, PSO, ACS, and P&O is 519.5 W, 519.2 W, 517.6 W, 518.7 W and 519.3 W. Maximum efficiency attained by WCA is 99.80%, DFO 99.75%, PSO 97.6%, ACS 98.7% and P&O has 99.4% respectively. The tracking time to WCA, DFO, PSO, ACS, and P&O is 0.19 s, 0.25 s, 0.41 s, 0.45 s, and 0.31 s. In tracking the global maxima, WCA is closed to DFO by 10 ms. WCA settle global maxima within 453 ms attaining 18% faster tracking which enriches its robustness and also removed unwanted fluctuations. Case 4 shows the best performance among other MPPT techniques. It can perceive and converge GM in fewer iterations.

Conclusion

In this research study, a novel technique has been designed for MPPT of PV system under different irradiance conditions. Proposed MPPT technique is tested under five different irradiance conditions and under all cases, it successfully find and track the global maxima to extract maximum power from PV system. In different stages of advancement of the paper, flow charts of all presented techniques, proposed technique pseudo code and Simulink/MATLAB are also presented. Then the proposed technique is compared with other well-known and widely used conventional technique P&O and a soft computing technique PSO. After thoroughly studying the results it has been proved that proposed WCA based technique shows better results in terms of convergence speed and efficiency over P&O and PSO while accuracy is found to be same as of PSO but better than P&O. Other performance criteria like, steady state oscillations, cost and complexity is same as of PSO. WCA based technique converges in significantly less time than PSO and after achieving steady state it retains zero oscillations. The robustness of the WCA has been verified under uniform and various partial shading conditions. WCA able to track the MPP accurately with good efficiency under the partial shading conditions and shows no oscillation after reaching the steady state.

References

Aouchiche, N., M. S. Aitcheikh, M. Becherif, and M. A. Ebrahim. 2018. AI-based global MPPT for partial shaded grid connected PV plant via MFO approach. *Solar Energy* 171: 593–603. doi:10.1016/j.solener.2018.06.109.

Babu, T. S., N. Rajasekar, and K. Sangeetha. 2015. Modified particle swarm optimization technique based maximum power point tracking for uniform and under partial shading condition. *Applied Soft Computing* 34:613–24. doi:10.1016/j.asoc.2015.05.029.

Bouselham, L., M. Hajji, B. Hajji, and H. Bouali. 2017. A new MPPT-based ANN for photovoltaic system under partial shading conditions. *Energy Procedia* 111:924–33. doi: 10.1016/j.egypro.2017.03.255.

Daraban, S., D. Petreus, and C. Morel. 2013. A novel global MPPT based on genetic algorithms for photovoltaic systems under the influence of partial shading. IECON Proceedings (Industrial Electronics Conference), 1490–1495.

Q2 Daraban, S., D. Petreus, and C. Morel. 2014. A novel MPPT (maximum power point tracking) algorithm based on a modified genetic algorithm specialized on tracking the global maximum power point in photovoltaic systems affected by partial shading. *Energy* 74 (C):374–88. doi:10.1016/j.energy.2014.07.001.

Eskandar, H., A. Sadollah, A. Bahreininejad, and M. Hamdi. 2012. Water cycle algorithm - A novel metaheuristic optimization method for solving constrained engineering optimization problems. *Computers and Structures* 110–111:151–66. doi:10.1016/j.compstruc.2012.07.010.

Ghaffarzadeh, N. 2015. Water Cycle Algorithm based power system stabilizer robust design for power systems. *Journal of Electrical Engineering* 66 (2):91–6. doi:10.1515/jee-2015-0014.

Ghasemi, M. A., H. M. Foroushani, and M. Parniani. 2016. Partial shading detection and smooth maximum power point tracking of PV arrays under PSC. *IEEE Transactions on Power Electronics* 31 (9):6281–92. doi:10.1109/TPEL.2015.2504515.

Haroon, S. S., and T. N. Malik. 2017. Short-term hydrothermal coordination using water cycle algorithm with evaporation rate. *International Transactions on Electrical Energy Systems* 27 (8):1–18.

Harrag, A., and S. Messalti. 2015. Variable step size modified P&O MPPT algorithm using GA-based hybrid offline/online PID controller. *Renewable and Sustainable Energy Reviews* 49:1247–60. doi:10.1016/j.rser.2015.05.003.

Ishaque, K., Z. Salam, A. Shamsudin, and M. Amjad. 2012. A direct control based maximum power point tracking method for photovoltaic system under partial shading conditions using particle swarm optimization algorithm. *Applied Energy* 99:414–22. doi:10.1016/j.apenergy.2012.05.026.

Karami, N., N. Moubayed, and R. Outbib. 2017. General review and classification of different MPPT Techniques. *Renewable and Sustainable Energy Reviews* 68:1–18. doi:10.1016/j.rser.2016.09.132.

Miyatake, M., M. Veerachary, F. Toriumi, N. Fujii, and H. Ko. 2011. Maximum power point tracking of multiple photovoltaic arrays: A PSO approach. *IEEE Transactions on Aerospace and Electronic Systems* 47 (1):367–80. doi:10.1109/TAES.2011.5705681.

Mohapatra, A., B. Nayak, P. Das, and K. B. Mohanty. 2017. A review on MPPT techniques of PV system under partial shading condition. *Renewable and Sustainable Energy Reviews* 80:854–67. doi:10.1016/j.rser.2017.05.083.

Punitha, K., D. Devaraj, and S. Sakthivel. 2013. Artificial neural network based modified incremental conductance algorithm for maximum power point tracking in photovoltaic system under partial shading conditions. *Energy* 62:330–40. doi:10.1016/j.energy.2013.08.022.

Ram, J. P., T. S. Babu, and N. Rajasekar. 2017. A comprehensive review on solar PV maximum power point tracking techniques. *Renewable and Sustainable Energy Reviews* 67: 826–47. doi:10.1016/j.rser.2016.09.076.

REN21. 2018. Renewables 2018 Global Status Report [Online]. http://www.ren21.net/wp-content/uploads/2018/06/17-8652_GSR2018_FullReport_web_final_.pdf (accessed December 26, 2018).

Sadollah, A., H. Eskandar, A. Bahreininejad, and J. H. Kim. 2015. Water cycle algorithm for solving multi-objective optimization problems. *Soft Computing* 19 (9):2587–603. doi: 10.1007/s00500-014-1424-4.

Villalva, M. G., J. R. Gazoli, and E. R. Filho. 2009. Modeling and circuit-based simulation
Q3 of photovoltaic arrays. 1244–54.

Villalva, M. G., J. R. Gazoli, and E. R. Filho. 2009. Comprehensive approach to modeling and simulation of photovoltaic arrays. *IEEE Transactions on Power Electronics* 24 (5): 1198–208. doi:10.1109/TPEL.2009.2013862.

Yilmaz, U., A. Kircay, and S. Borekci. 2018. PV system fuzzy logic MPPT method and PI control as a charge controller. *Renewable and Sustainable Energy Reviews* 81:994–1001. doi:10.1016/j.rser.2017.08.048.

Zhang, J., K. Ding, R. Mei, and Y. Cai. 2018. Global maximum power point tracking method based on sorting particle swarm optimizer. *International Journal of Green Energy*
Q4 15 (13):821–36. doi:10.1080/15435075.2018.1529579.